Finite element analysis of crenulated and non-crenulated hominid molars : A functional hypothesis explaining the adaptive significance of molar crenulation

Cano-Fernandez, Hugo

2022-04

Cano-Fernandez , H & Jernvall , J 2022 , ' Finite element analysis of crenulated and non-crenulated hominid molars : A functional hypothesis explaining the adaptive significance of molar crenulation ' , American journal of biological anthropology , vol. 177 , no. 4 , pp. 760-768 . https://doi.org/10.1002/ajpa.24472

http://hdl.handle.net/10138/353779
https://doi.org/10.1002/ajpa.24472

unspecified
acceptedVersion

Finite element analysis of crenulated and non-crenulated human molars: a functional hypothesis explaining the adaptive significance of molar crenulation.

Hugo Cano-Fernandez, Jukka Jernvall

1. Autonomic University of Barcelona
2. University of Helsinki, Institute of Biotechnology, Developmental Biology Program, Helsinki, Finland

- Corresponding author: Hugo Cano-Fernandez (hugo.cano@telefonica.net)

Abstract

Objectives: The occlusal surface of many mammalian teeth has grooves that have been collectively called crenulations. The evolutionary significance of this trait is unknown, but it has been associated with a hard diet. It has not been explained, however, why crenulated molars may present an increased mechanical resistance. The objective of this study was to determine whether a crenulated surface dissipate mechanical stress more efficiently than a smooth one.
Materials and Methods: Using μCT scans we built 3D models of lower second molars from *Homo*, *Pan*, *Gorilla* and *Pongo*. The crenulated models from *Homo* and *Pongo* were modified to remove crenulations. Finite element analysis was used to determine the distribution of mechanical stress in all the models when a vertical force was applied.
Results: The results show that crenulated molars have a distinctive pattern of mechanical stress, namely the stress is higher in the valleys than in the crests of the crenulations. In non-crenulated molars, mechanical stress is more homogeneously distributed. Highly crenulated molars of orangutans show the smallest values of mean stress among the compared species. Artificially removing crenulations results in more homogeneous distribution of stresses and increased mean stress values.
Discussion: Molar crenulations may increase molar resistance by canalizing mechanical stress from the tip to the base of the cusps. The overall cusp shape also influences the distribution of stress. This mechanism may be a functional hypothesis to explain the association between crenulated molars and mechanically demanding diets.

Introduction

Teeth are central to the study of human and primate evolution because they are the most common and well preserved fossils. They show very variable morphologies that have been used for taxonomic identification and phylogenetic reconstruction (Berger et al., 2015; Haile-Selassie, 2001; Senut, Pickford, & Gommery, 2018; Silcox, 2001). Tooth shape has been frequently associated with diet and changes in it are usually interpreted as

adaptations to exploit food resources (Berthaume, Delezene, & Kupczik, 2018; Boyer, Evans, & Jernvall, 2010; Ledogar, Winchester, St. Clair, & Boyer, 2013; Thiery, Guy, & Lazzari, 2017).

Molar crenulation is a sometimes overlooked aspect of dental variation which has been defined as the presence of secondary well-defined cristids in each molar cusp (Grine, 1981; Swindler & Ward, 1988). This trait is present in living primates such as orangutans, chimpanzees, gorillas (Kraus & Oka, 1967), bamboo lemurs (Eronen et al., 2017), and pitheciines (Ledogar et al., 2013); as well as in some populations of modern humans (Grine, 1981; Pilloud, Maier, Scott, & Edgar, 2018). In addition, it has also been frequently described in hominin (Berger et al., 2015; Bermúdez de Castro, Rosas, & Nicolaás, 1999; Frayer, 1973; Haile-Selassie, 2001; Martinón-Torres, Castro, Gómez-Robles, Prado-Simón, & Arsuaga, 2012; Pickering et al., 2016; Simpson et al., 2015; Tobias, 1967; Xing, Martinón-Torres, & Castro, 2018; Xing et al., 2016) and primate fossils (Beard et al., 2009; Chaimanee et al., 2003; Coster et al., 2013; Godinot, 2014; Kay et al., 2004; Silcox, 2001; Zhang et al., 2014).

Despite being ubiquitously present in primate and human evolution, the developmental origin and evolutionary meaning of enamel crenulation remain unclear. It has been shown using CT-scans that the topology of the outer enamel surface (OES), and therefore the presence of enamel crenulations, is largely determined by the enamelodentinary junction (EDJ). However, the topology of the OES cannot always be predicted as a geometric projection of the EDJ (Skinner et al., 2010). Developmental modeling suggest that slightly curved areas of the EDJ can create a lack of nutrients in ameloblasts during the secretion stage, leading to a differential pattern of enamel deposition. This process is nonlinear, meaning that small changes in the initial conditions can create large changes in the topology of the OES (Häkkinen et al., 2019). The close relationship between the OES and the EDJ and the lack of statistical association between the complexity of the crenulation pattern and the percentage of fruit in diet have led to propose that molar crenulations are just a by-product of development with no adaptive meaning (Cano-Fernández & Gómez-Robles, 2021).

The OES topology has traditionally been associated to diet because teeth are used for food pre-processing. Many of the primates that present molar crenulations, such as great apes, feed primarily on ripe fruits (Constantino, Lucas, Lee, & Lawn, 2009; Ledogar et al., 2013; Martin, Olejniczak, & Maas, 2003; Vogel et al., 2008). Molar crenulations often resemble the grooves and crests of a squeezer and, therefore, it may be proposed that they can be used to extract the juice of fruits. However, it has never been experimentally tested whether juicing fruits has any adaptive advantage over slicing them and a clear correlation between fruit consumption and the expression of molar crenulations has not been found (Berthaume, Lazzari, & Guy, 2020; Cano-Fernández & Gómez-Robles, 2021).

Primates that present molar crenulations often rely on of hard items such as unripe fruits, seeds, culm or barks when their main food resources are not available (Constantino et al., 2009; Eronen et al., 2017; Kay, 1981; Ledogar et al., 2013; Martin et al., 2003; Vogel et al., 2008). This trait has therefore been associated with a hard diet in two not exclusive ways. Firstly, accessory crests (or cristids) in molar occlusal surface may be used to trap the small

and hard food particles, such as seeds. These sharp crests also present a small contact surface increasing the mechanical stress produced in the food particles (Lucas & Luke, 1984). Secondly, it has been suggested that grooves, fissures and crests in the enamel occlusal surface may direct the tensile stresses from the cusps to the centre of the molars making them more resistant (Benazzi, Kullmer, Grosse, & Weber, 2011).

The objective of this study was to use the well established methodology of finite element analysis (Berthaume et al., 2010; Commisso, Martínez-Reina, Ojeda, & Mayo, 2015; Habegger et al., 2020; Kupczik & Chattah, 2014; Ledogar, Luk, Perry, Neaux, & Wroe, 2018; Smith et al., 2015; Stansfield, Parker, & O'Higgins, 2018) to explore the role of enamel crenulations in molar resistance and the distribution of mechanical stress in the OES. Although it has been already suggested that grooves in the OES may be able to canalize mechanical stress (Benazzi et al., 2011), this hypothesis has never been tested using models of molars with and without crenulations. The second goal of this study was to compare the pattern of mechanical stress distribution in the OES between crenulated and non-crenulated primate molars from different species under similar loads.

Materials and Methods

Materials

Microcomputed tomography scans (μCT) of second lower molars from great apes and humans were used in this study to create 3D models and assess the distribution of mechanical stress. The human μCT scans were downloaded from two different sources: the ESRF heritage database (http://paleo.esrf.fr/picture.php?/159/category/467) and the Morphosource database. The modern human molar from the ESRF heritage database (EQ-H5) was downloaded as a set of raw μCT scan images and it was a fossil found in the Equus Cave in South Africa dating back to 33,000-94,000 years before present (Grine & Klein, 1985; Smith et al., 2006). The details of the scanning procedure of this fossil were described in Smith et al. (2006). The human molar from Morphosource was scanned at the Duke University and it was downloaded as a surface file (ark:/87602/m4/M109383). The great ape μCT scans came from the American Museum of Natural History and they were also downloaded as surface files from Morphosource. The sample included a highly crenulated molar from *Pongo pygmaeus* (ark:/87602/m4/M18425), and two non-crenulated molars from *Pan troglodytes* (ark:/87602/m4/M18117) and *Gorilla gorilla* (ark:/87602/m4/M17146).

Modified 3D models

The modern human molar EQ-H5 and the orangutan molar were used to test the effect in the distribution of mechanical stress of removing enamel crenulations. These molars were selected because they present very clear crenulations. In the case of the human molar EQ-H5, the raw μCT scans were used to create a model with crenulations corresponding to the original morphology where only the taphonomic fractures in the fossil were sealed. Then, the crenulations were manually filled in in the slices using the software ImageJ. The result

was a 3D model retaining the overall cusp shape and the main grooves between cusps, but with no secondary crests or valleys. These models were built with squared voxels of 0.0649mm using the software VOX-FE (Banglawala, Bethunel, Fagan, & Holbrey, 2015). The crenulated model included 1,949,910 voxels and the non-crenulated model 2,025,200 voxels.

The surface mesh of the orangutan molar was processed using the software Meshlab. The number of elements in the mesh was reduced using the quadratic edge collapse decimation until the OES was represented by five thousand vertices. The holes in the meshes were repaired using the "Close holes" function and the HC Laplacian smoothing was applied once to reduce the irregularities produced by the mesh simplification (Vollmer, Mencl, & Mueller, 1999). Three models without crenulations were created by smoothing the OES using the HC Laplacian algorithm three, six and ten times more respectively. The three representations of the OES were imported to the software FreeCad and converted into solid meshes using the program gmsh 4.8.1 (Geuzaine & Remacle, 2009) with a maximum element size between 0.40 and 0.23mm and a minimum element size of 10μm. The resulting finite element meshes had approximately between 240,000 and 450,000 elements.

The distribution of mechanical stress in naturally non-crenulated molars was assessed using the human, chimpanzee and gorilla molars. The surface files downloaded from Morphosource were also processed using the quadratic edge collapse decimation, the "Close holes" and the HC Laplacian smoothing functions in the software Meshlab. The resulting surface meshes were imported to FreeCad and finite element meshes ranging from 177,000 to 350,000 elements were built using gmsh 4.8.1 with a maximum element size between 0.36 and 0.23mm and a minimum element size of 10μm.

Material properties

Great apes and humans have different values of enamel thickness and both the enamel thickness and the topology of the EDJ affect the dissipation of mechanical stress (Imbeni, Kruzic, Marshall, Marshall, & Ritchie, 2005; Shellis, Beynon, Reid, & Hiiemae, 1998). To avoid different enamel thicknesses or EDJ topology affecting our results on the patterns of mechanical stresses in the OES, we assumed the molar volume to be made of enamel. The physical properties of enamel are variable in different areas of the molar and they may also be different between species (An, Wang, Arola, & Zhang, 2012; Manly, Hodge, & Ange, 1939). For the sake of simplicity, however, if was assumed that enamel is homogeneous and it has a the Young's modulus of 95GPa, a Poisson's ratio of 0.3 and a density equal to $2.80 g/c\,m^3$ (Kupczik & Chattah, 2014; Weidmann, Weatherell, & Hamm, 1967). Overall, the strict focus on the OES patterns should provide a first approximation of the role significance of crenulations in primate dentition.

Physical constraints

The distribution of mechanical stresses was calculated simulating vertical forces applied to the tips of the cusps. In the crenulated and non-crenulated models obtained from human molar EQ-H5, forces of 72N (Kupczik & Chattah, 2014) were distributed homogeneously

among a total number of 144 and 138 nodes respectively, while the basal nodes were constrained so that they could not move in the z axis. These two models were solved using the software VOX-FE and the stress was measured as the principal component of mechanical stress (P1) (Banglawala et al., 2015).

In the rest of the crenulated and non-crenulated molars from great apes and humans pressures of 20MPa were applied to the tips of the cusps. The total surface of molar cusp tips was larger in larger molars, therefore applying pressures allowed to normalize the total force applied by the size of the molars. The basal nodes were also constrained so that the could not move. The models were solved using the software Calculix and the stress was measured as the Von Mises stress.

Results

The finite element analysis in the fossil human molar EQ-H5 yielded different patterns of distribution of mechanical stress in the crenulated and non-crenulated models. In the crenulated model the mechanical stress was higher in the in the valleys than in the crests of the secondary grooves, whereas in the non-crenulated model the distribution of mechanical stress was more homogeneous (*Figure 1.*). The maximum values of the principal component of mechanical stress and displacement on the occlusal surface were higher in the non-crenulated than in the crenulated model (*Table 1.*).

To test this further, a local analysis was performed in one of the cusps (protoconid) that presents clear crenulations. Two areas were selected corresponding to the surface of one crest and its corresponding valley of the crenulation. The values of P1 in the selected points were aggregated by height (z) intervals of 0.1mm to obtain a representation of how the mechanical stress is transmitted from the tip to the base of the cusps. The mean values are represented in *Figure 1.E* and they show that stress is effectively larger in the valley than in the crest.

The cusp shape, and not only the crenulations, may be responsible for the differences in the P1 values found between adjacent areas. The effect of general cusp shape was tested by selecting surfaces in the non-crenulated model homologous that can be considered as homologous to the valley and crest of the crenulated model and measuring the average P1 values in each 0.1mm height interval. The results (*Figure 1.F*) show that the valleys have slightly higher P1 values compared to the ridges. Nevertheless, the P1 values in the valley of the crenulated molars were still higher than those in the valleys of the non-crenulated molar.

The pattern of mechanical stress was also different in the crenulated and non-crenulated models of the orangutan molar, the latter obtained by smoothing the crenulated shapes. Again, the crenulated model showed larger values of stress in the valleys of the crenulations than in the cristids whereas in the smoothed molars the stress was distributed homogeneously (*Figure 2.*). The mean value of Von Mises stress and displacement on the basin surface was also smaller in the crenulated than in the non-crenulated models (*Table 2.*). The pattern of distribution of mechanical stress was homogeneous in the naturally non-

crenulated molars from *Homo*, *Pan* and *Gorilla*. The maximum values of Von Mises stress on the occlusal surface were smaller the molars from *Pongo* and *Homo* molar than in *Pan* and *Gorilla*. The mean values of Von Mises stress and total displacement were smaller in *Pongo* than in the rest of the species (*Table 3*).

Discussion

The biomechanical meaning of molar crenulations

In this study the finite element analysis methodology was used to measure the distribution of mechanical stress in the OES of crenulated and non-crenulated molars when a perpendicular force is applied. The results obtained from models of great ape and humans molars show that molar crenulation create a distinctive pattern of mechanical stress. In crenulated molars the mechanical stress is higher in the valleys than in the crests, whereas in non-crenulated molars the stress is distributed homogeneously. The role of overall cusp morphology was further tested by measuring the mean stress values in 0.1mm intervals from the tip to the base of the cusp in the crests and valleys of one cusp in the EQ-H5 crenulated and non-crenulated models. For the same height intervals, the stress values were higher in the valley than in the crest in both crenulated and non-crenulated models, although the difference was larger in the crenulated model. This suggests that the overall shape of the cusp also has some effect into the distribution of mechanical stress. The accumulation of mechanical stress in the valleys of the OES had previously been observed in models from human molars (Benazzi et al., 2011), but it had never been assessed in model of the same molar with and without crenulations.

The two methodologies used to remove the molar crenulations yielded similar results in terms of resistance indicators. Filling in the crenulations manually in the μCT scans resulted in a decrease in the maximum and mean values of mechanical stress and displacement on the occlusal surface. These results support that molar crenulations increase resistance at the level of the OES. Smoothing the cusps in the orangutan molar with the HC Laplacian algorithm yielded an increase of both average mechanical stress and displacement in the basin. The maximum Von Mises stress in the basin lacked a clear trend (*Table 2*), reflecting the rounding of the cusp tips. The HC Laplacian algorithm substitutes the position of every point of the surface mesh by the average of the position of the adjacent vertices (Vollmer et al., 1999). The first time that the algorithm was applied it successfully removed the imperfections in the models due to random sampling of the raw data. When this algorithm was repeatedly applied to the orangutan molar, the crenulations disappeared, but the cusps also become more low and blunt. It has been noticed that blunt cusps are an optimal morphology to crack hard food items because they act like a pestle and mortar (Lucas & Luke, 1984). This may explain the reduction in the Von Mises stress and displacement values that was observed in cusp tips of the orangutan molars. Overall, whereas comparisons of finite element models that differ in size and shape entail many challenges (Dumont et al., 2009), the generally similar effects of the smoothing on the patterns of stress should be at least suggestive about the functional significance of crenulations.

Molar crenulation and diet in primates

The mean values of mechanical stress were lower in orangutans than in humans, chimpanzees and gorillas. Although these models may not be entirely comparable due to the differences in size and overall shape of the molar cusps, these results are consistent with the interpretation that enamel crenulations increase molar resistance and, therefore, this trait may be a dietary adaptation in species that rely on hard nutritional items (Kay, 1981). Molar crenulation is frequent in primates species with a diet that includes hard items such as orangutans, chimpanzees, gorillas, pitheciines and bamboo lemurs (Constantino et al., 2009; Eronen et al., 2017; Ledogar et al., 2013; Vogel et al., 2008).

The primary dietary resource of great apes is ripe fruit, but when it is scarce they rely on secondary nutritional sources that can include hard items. Orangutans consume seeds and unripe fruit when there is no ripe fruit. Gorillas rely on herbaceous terrestrial vegetation, which is a tough material, but they also consume barks, which are a hard item. Chimpanzees, however, present a more varied diet, searching for more ripe fruit or herbaceous terrestrial vegetation when the primary resources are scarce. (Constantino et al., 2009; Vogel et al., 2008). Similarly, although the greater bamboo lemur consumes bamboo leaves almost throughout the year, mechanically challenging bamboo shoots and culm are the principal diet during several months (Eronen et al., 2017).

Pitheciines represent an extreme case of molar crenulation that has been interpreted as an adaptation to consume seeds and unripe fruit, which are the basis of the diet in this group (Ledogar et al., 2013). Indeed, it has also been shown using finite element analysis that the morphology of their skulls is adapted to dissipate the internal loads during mastication (Ledogar et al., 2018). In addition, the enamel of these primates presents a high prism decussation, which may also be responsible for an increase molar resistance. However, the enamel of pitheciine molars is thin, therefore, it can also be interpreted that they actually use their strong canines and incisors to break the hard seed coat, whereas the molars are only used to masticate the soft inner layers of seeds (Martin et al., 2003).

The expression of molar crenulations is less conspicuous in modern humans than in orangutans or pitheciines (Cano-Fernández & Gómez-Robles, 2021; Kraus & Oka, 1967), although some examples of highly crenulated human molars can be found in African and Asian populations (Grine, 1981; Pilloud et al., 2018). Highly crenulated molars also appear frequently in the hominin fossil record (Berger et al., 2015; Bermúdez de Castro et al., 1999; Frayer, 1973; Haile-Selassie, 2001; Martinón-Torres et al., 2012; Pickering et al., 2016; Simpson et al., 2015; Tobias, 1967; Xing et al., 2018). If the dietary hypothesis of molar crenulation is correct (Kay, 1981), then the reason why the frequency of molar crenulation has been reduced during human evolution may be related to a decrease in the amount of hard items in diet that led to a relaxation of the selection pressure in this trait. Cooking and an increase in meat consumption may be tentatively pointed as determinant drivers of this process. Alternatively, if molar crenulation is only a byproduct of development with no significant functional effects (Cano-Fernández & Gómez-Robles, 2021), then this trait may have been lost in human evolution due to genetic drift.

A functional hypothesis for molar crenulations

The distinctive pattern of mechanical stress that was found in the molars of *Homo* and *Pongo* suggest that crenulations may canalize mechanical stresses from the tips to the base of the molar cusps, as it has been suggested in a previous study (Benazzi et al., 2011). This may increase resistance in a similar way than the buttresses increase stability in buildings (Thipparthi, Kandalai, & Kiran, 2021). Although our results are preliminary and should be validated in a larger sample, we can propose that the canalization of forces at the level of the outer enamel surface is a new hypothesis to explain why crenulated molars may present an increased mechanical resistance. This explanation could also shed light on the traditionally acknowledged association between this trait and a hard diet in primates.

Further research is required to clarify whether crenulated molars are indeed more resistant and whether this trait may has been selected positively in the evolution of primate groups which frequently include hard items in their diet, such as pitheciines, bamboo lemurs or orangutans. New studies may include more complete finite element models considering not only enamel, but also dentin and alveolar bone. Finally, understanding the biomechanical properties of crenulated and non-crenulated molars is vital to establish correct dietary inferences in fossil mammal species (Candela, Cassini, & Nasif, 2013; Kay et al., 2004; Martin et al., 2003).

Conclusions

In this study, the well-established methodology of finite element analysis has been used to test whether the distribution of mechanical stresses in the enamel surface is different in crenulated and non-crenulated molars from great apes and humans when a perpendicular force is applied. Our results point that enamel crenulations may be able to canalize stress from the tip to the base of the molar cusps, increasing molar resistance. Although more research is needed to confirm these findings, this constitutes a functional hypothesis to explain why crenulated molars may be more resistant than non-crenulated ones and, consequently, the traditionally proposed correlation between this trait and the presence of hard items in the diet in primates.

Data availability statement

The CT-scans used in this study are freely available online on the ESRF heritage database for palaeontology, evolutionary biology and archaeology (http://paleo.esrf.fr/) and Morphosource (https://www.morphosource.org/). The models and the rest of the data that support our findings are available from the corresponding author, H.C.-F., upon reasonable request.

Acknowledgments

We are grateful to the ESRF heritage database for palaeontology, evolutionary biology and archaeology and the Morphosource database that offer free access to the CT-scans used in this study. We also want to thank professors Isaac Salazar-Ciudad and José Manuel Cano-Izquierdo and the two anonymous reviewers for their useful comments.

Funding

This research has been funded by the Finnish Academy. The Morphosource scans were imaged thanks to the A Leakey Foundation Grant and NSF BCS 1304045 awarded to E. St. Clair and D. M. Boyer and NSF BCS 1552848 to D. M. Boyer.

Figures

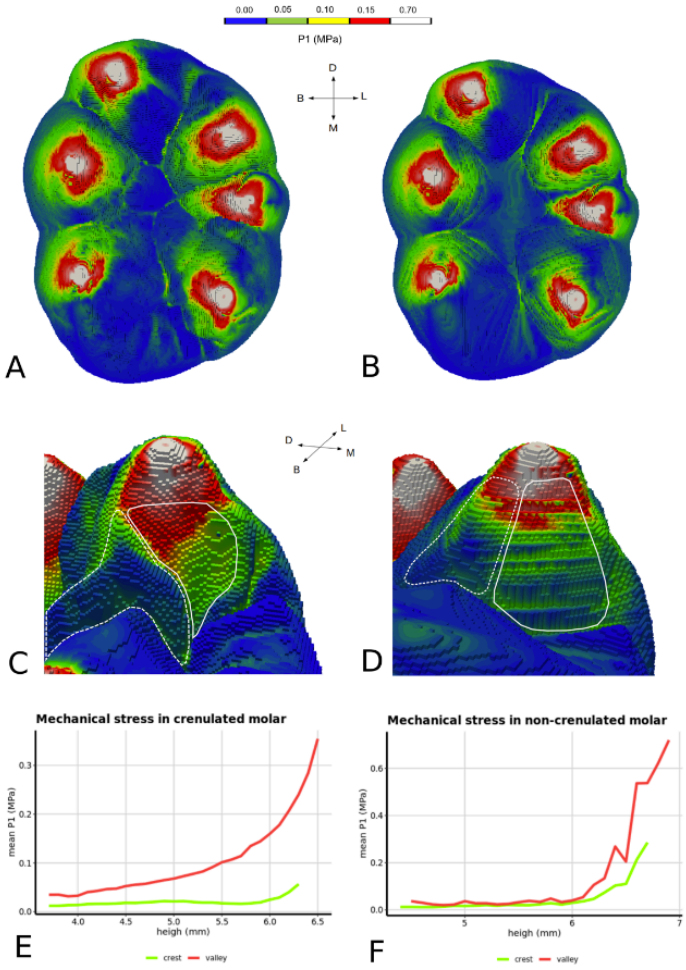

Figure 1. Results of the crenulated and non-crenulated models of the human molar EQ-H5. Heatmap showing the values of the maximum principal stress (P1) in the crenulated (A)

and non-crenulated (B) models. Detail of the heatmap showing the values P1 in one molar cusp for the crenulated (C) and non-crenulated (D) models. In the crenulated model (C) the continuous polygon shows the crest and the slashed polygon the valley of one crenulation. In the non-crenulated model (D) the polygons show the homologous surfaces to the crest (continuous) and the valley (slashed). (E) Plot showing the average values of P1 in the crest and the valley of the image C aggregated in intervals of 0.1mm of height. (F) Plot showing the average values of P1 in the homologous surfaces of the image D aggregated in intervals of 0.1mm of height.

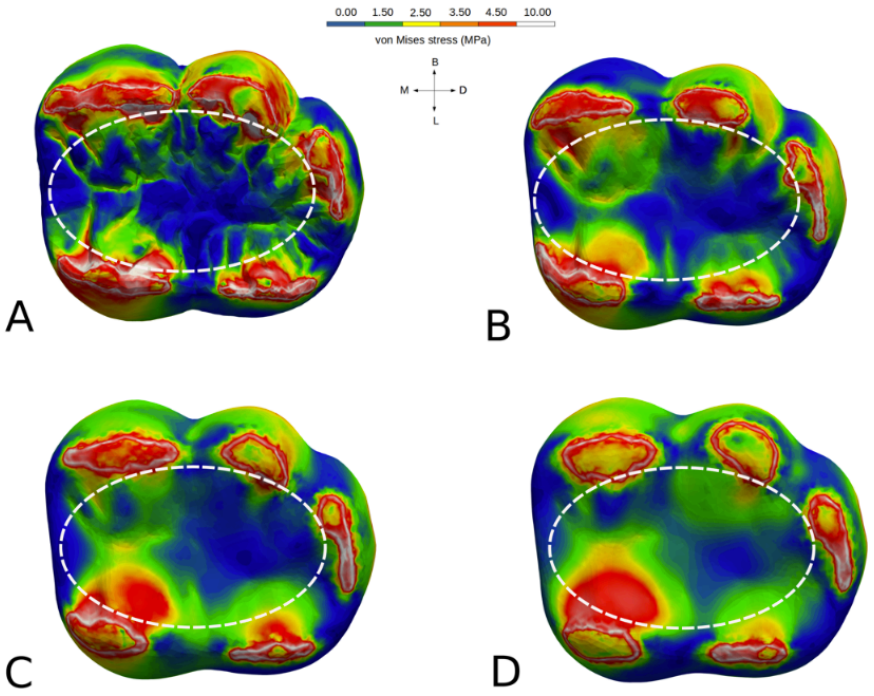

Figure 2. Heatmaps showing the distribution of the Von Mises stress in the different models obtained from the orangutan second lower molar under a load of 20MPa in each molar cusp. The ellipses delineate the area of the basin from which the stresses are listed in *Table 2.* (A) Original molar where outer enamel surface (OES) has been smoothed once with the HC Laplacian algorithm to remove irregularities in the random sampling of the raw data. (B) Model where the OES has been smoothed 4 times to remove crenulations. (D) Model where the OES has been smoothed 7 times to remove crenulations. (C) Model where the OES has been smoothed 11 times to remove crenulations.

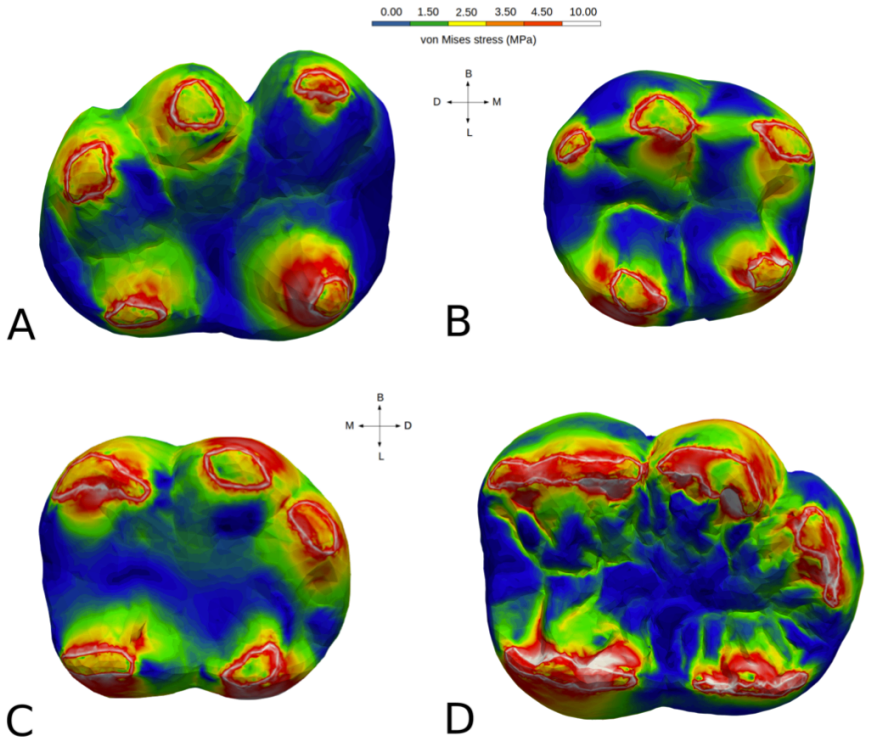

Figure 3. Heatmaps showing the distribution of the Von Mises stress in the naturally non-crenulated molars from *Gorilla gorilla* (A), *Homo sapiens* (B), *Pan troglodytes* (C) and the highly crenulated molar from *Pongo pygmaeus* (D) under a load of 20MPa in each molar cusp.

Tabels

Table 1. Results of the crenulated and non-crenulated models of the human molar EQ-H5. Mean displacements in μm in each axis (x, y, z) and total displacement (TDis) with standard deviations (sdx, sdy, sdz), mean maximum principal stress (P1) in MPa with its standard deviation (sd P1), maximum P1 (max P1) and the number of nodes selected (N) in the occlusal surface.

Model	x	sdx	y	sdy	z	sdz	TDis	P1	sd P1	max P1	N
crenulated	-13.729	101.938	15.161	87.695	-228.925	273.904	256.529	0.069	0.28	12.002	91207
non-crenulated	-11.655	109.512	20.459	87.772	-276.678	304.479	299.853	0.088	0.342	13.668	61431

Table 2. Results in the basin surface of the crenulated and non-crenulated orangutan models. Mean displacements in μm in each axis (x, y, z) and total displacement (TDis) with standard deviations (sdx, sdy, sdz), mean Von Mises stress (Von Mises) in MPa with its standard deviation (sd Von Mises), maximum Von Mises stress (max Von Mises) and the number of nodes selected (N) in the occlusal surface.

Times smoothed	x	sdx	y	sdy	z	sdz	TDis	Von Mises	sd Von Mises	max Von Mises	N
1	0.01	0.011	-0.005	0.01	0.005	0.011	0.015	1.008	0.848	8.401	12922
4	-0.001	0.006	-0.008	0.016	0.01	0.018	0.02	1.389	1.062	5.987	7809
7	-0.001	0.013	0.002	0.011	0.009	0.017	0.018	1.424	1.092	9.659	4543
11	0.001	0.016	0.007	0.021	0.009	0.019	0.023	1.743	1.307	8.002	4266

Table 3. Results of great ape and human models. Mean displacements in μm in each axis (x, y, z) and total displacement (TDis) with standard deviations (sdx, sdy, sdz), mean Von Mises stress (Von Mises) in MPa with its standard deviation (sd Von Mises), maximum Von Mises stress (max Von Mises) and the number of nodes selected (N) in the occlusal surface.

Genus	x	sdx	y	sdy	z	sdz	TDis	Von Mises	sd Von Mises	max Von Mises	N
Homo	0.033	0.049	0.026	0.037	0.055	0.052	0.079	2.808	1.89	13.781	33135
Pan	0.018	0.047	-0.02	0.034	-0.046	0.07	0.068	3.116	2.424	29.195	40981
Gorilla	-0.009	0.028	-0.004	0.068	0.043	0.07	0.072	2.827	2.39	24.896	25006
Pongo	0.019	0.026	-0.003	0.021	0.031	0.051	0.056	2.189	2.174	15.438	39146

Bibliography

An, B., Wang, R., Arola, D., & Zhang, D. (2012). The role of property gradients on the mechanical behavior of human enamel. *Journal of the Mechanical Behavior of Biomedical Materials*, *9*, 63–72.

Banglawala, N., Bethunel, I., Fagan, M., & Holbrey, R. (2015). Voxel-based finite element modelling with VOX-FE2. *White Paper Funded Under the Embedded CSE Programme of the ARCHER UK National Supercomputing Service*.

Beard, K. C., Marivaux, L., Chaimanee, Y., Jaeger, J.-J., Marandat, B., Tafforeau, P., … Kyaw, A. A. (2009). A new primate from the Eocene Pondaung Formation of Myanmar and the monophyly of Burmese amphipithecids. *Proceedings of the Royal Society B: Biological Sciences*, *276*(1671), 3285–3294.

Benazzi, S., Kullmer, O., Grosse, I. R., & Weber, G. W. (2011). Using occlusal wear information and finite element analysis to investigate stress distributions in human molars. *Journal of Anatomy*, *219*(3), 259–272.

Berger, L. R., Hawks, J., Ruiter, D. J. de, Churchill, S. E., Schmid, P., Delezene, L. K., … others. (2015). *Homo naledi*, a new species of the genus *homo* from the Dinaledi Chamber, South Africa. *Elife*, *4*, e09560.

Bermúdez de Castro, J. M., Rosas, A., & Nicolaás, M. E. (1999). Dental remains from Atapuerca-TD6 (Gran Dolina site, Burgos, Spain). *Journal of Human Evolution*, *3*(37), 523–566.

Berthaume, M. A., Delezene, L. K., & Kupczik, K. (2018). Dental topography and the diet of *homo naledi*. *Journal of Human Evolution*, *118*, 14–26.

Berthaume, M. A., Lazzari, V., & Guy, F. (2020). The landscape of tooth shape: Over 20 years of dental topography in primates. *Evolutionary Anthropology: Issues, News, and Reviews*, *29*(5), 245–262.

Berthaume, M., Grosse, I. R., Patel, N. D., Strait, D. S., Wood, S., & Richmond, B. G. (2010). The effect of early hominin occlusal morphology on the fracturing of hard food items. *The Anatomical Record: Advances in Integrative Anatomy and Evolutionary Biology*, *293*(4), 594–606.

Boyer, D. M., Evans, A. R., & Jernvall, J. (2010). Evidence of dietary differentiation among late Paleocene–early Eocene plesiadapids (Mammalia, Primates). *American Journal of Physical Anthropology*, *142*(2), 194–210.

Candela, A. M., Cassini, G. H., & Nasif, N. L. (2013). Fractal dimension and cheek teeth crown complexity in the giant rodent *eumegamys paranensis*. *Lethaia*, *46*(3), 369–377.

Cano-Fernández, H., & Gómez-Robles, A. (2021). Assessing complexity in hominid dental evolution: Fractal analysis of great ape and human molars. *American Journal of Physical Anthropology*, *174*(2), 352–362.

Chaimanee, Y., Jolly, D., Benammi, M., Tafforeau, P., Duzer, D., Moussa, I., & Jaeger, J.-J. (2003). A Middle Miocene hominoid from Thailand and orangutan origins. *Nature*, *422*(6927), 61–65.

Commisso, M. S., Martínez-Reina, J., Ojeda, J., & Mayo, J. (2015). Finite element analysis of the human mastication cycle. *Journal of the Mechanical Behavior of Biomedical Materials*, *41*, 23–35.

Constantino, P. J., Lucas, P. W., Lee, J. J.-W., & Lawn, B. R. (2009). The influence of fallback foods on great ape tooth enamel. *American Journal of Physical Anthropology*, *140*(4), 653–660.

Coster, P., Beard, K. C., Soe, A. N., Sein, C., Chaimanee, Y., Lazzari, V., … Jaeger, J.-J. (2013). Uniquely derived upper molar morphology of Eocene Amphipithecidae (Primates: Anthropoidea): homology and phylogeny. *Journal of Human Evolution*, *65*(2), 143–155.

Dumont, E. R., Grosse, I. R., Slater & G. S. (2009) Requirements for comparing the performance of finite element models of biological structures. *Journal of Theoretical Biology* 256, 96– 103.

Eronen, J. T., Zohdy, S., Evans, A. R., Tecot, S. R., Wright, P. C., & Jernvall, J. (2017). Feeding ecology and morphology make a bamboo specialist vulnerable to climate change. *Current Biology*, *27*(21), 3384–3389.

Frayer, D. W. (1973). *Gigantopithecus* and its relationship to *australopithecus*. *American Journal of Physical Anthropology*, *39*(3), 413–426.

Geuzaine, C., & Remacle, J.-F. (2009). Gmsh: A 3-d finite element mesh generator with built-in pre-and post-processing facilities. *International Journal for Numerical Methods in Engineering*, *79*(11), 1309–1331.

Godinot, M. (2014). Fossil record of the primates from the Paleocene to the Oligocene. In W. Henke & I. Tattersall (Eds.), *Handbook of paleoanthropology: Vol II: Primate evolution and human origins* (pp. 1–102). Berlin: Springer.

Grine, F. E. (1981). Occlusal morphology of the mandibular permanent molars of the South African Negro and the Kalahari San (Bushman). *Annals of the South African Museum*, *86*(5), 157–215.

Grine, F. E., & Klein, R. G. (1985). Pleistocene and Holocene human remains from Equus cave, South Africa. *Anthropology*, *8*, 55–98.

Habegger, L., Motta, P., Huber, D., Pulaski, D., Grosse, I., & Dumont, E. (2020). Feeding biomechanics in billfishes: Investigating the role of the rostrum through finite element analysis. *The Anatomical Record*, *303*(1), 44–52.

Haile-Selassie, Y. (2001). Late Miocene hominids from the middle Awash, Ethiopia. *Nature*, *412*(6843), 178–181.

Häkkinen, T. J., Sova, S. S., Corfe, I. J., Tjäderhane, L., Hannukainen, A., & Jernvall, J. (2019). Modeling enamel matrix secretion in mammalian teeth. *PLoS Computational Biology*, *15*(5), e1007058.

Imbeni, V., Kruzic, J., Marshall, G., Marshall, S., & Ritchie, R. (2005). The dentin–enamel junction and the fracture of human teeth. *Nature Materials*, *4*(3), 229–232.

Kay, R. F. (1981). The nut-crackers–a new theory of the adaptations of the Ramapithecinae. *American Journal of Physical Anthropology*, *55*(2), 141–151.

Kay, R. F., Schmitt, D., Vinyard, C. J., Perry, J. M., Shigehara, N., Takai, M., & Egi, N. (2004). The paleobiology of Amphipithecidae, south Asian late Eocene primates. *Journal of Human Evolution*, *46*(1), 3–25.

Kraus, B. S., & Oka, S. W. (1967). Wrinkling of molar crowns: New evidence. *Science*, *157*(3786), 328–329.

Kupczik, K., & Chattah, N. L.-T. (2014). The adaptive significance of enamel loss in the mandibular incisors of cercopithecine primates (Mammalia: Cercopithecidae): A finite element modelling study. *PloS One*, *9*(5).

Ledogar, J. A., Luk, T. H., Perry, J. M., Neaux, D., & Wroe, S. (2018). Biting mechanics and niche separation in a specialized clade of primate seed predators. *PloS One*, *13*(1), e0190689.

Ledogar, J. A., Winchester, J. M., St. Clair, E. M., & Boyer, D. M. (2013). Diet and dental topography in pitheciine seed predators. *American Journal of Physical Anthropology*, *150*(1), 107–121.

Lucas, P., & Luke, D. (1984). Chewing it over: Basic principles of food breakdown. In *Food acquisition and processing in primates* (pp. 283–301). Springer.

Manly, R. S., Hodge, H. C., & Ange, L. E. (1939). Density and refractive index studies of dental hard tissues: II. Density distribution curves 1, 2. *Journal of Dental Research*, *18*(3), 203–211.

Martin, L. B., Olejniczak, A. J., & Maas, M. C. (2003). Enamel thickness and microstructure in pitheciin primates, with comments on dietary adaptations of the middle Miocene hominoid *kenyapithecus*. *Journal of Human Evolution*, *45*(5), 351–367.

Martinón-Torres, M., Castro, J. M. B. de, Gómez-Robles, A., Prado-Simón, L., & Arsuaga, J. L. (2012). Morphological description and comparison of the dental remains from Atapuerca-Sima de los Huesos site (Spain). *Journal of Human Evolution*, *62*(1), 7–58.

Pickering, T. R., Heaton, J. L., Sutton, M. B., Clarke, R. J., Kuman, K., Senjem, J. H., & Brain, C. (2016). New Early Pleistocene hominin teeth from the Swartkrans formation, South Africa. *Journal of Human Evolution*, *100*, 1–15.

Pilloud, M., Maier, C., Scott, G., & Edgar, H. (2018). Molar crenulation trait definition and variation in modern human populations. *Homo*, *69*(3), 77–85.

Senut, B., Pickford, M., & Gommery, D. (2018). Dental anatomy of the early hominid, *orrorin tugenensis*, from the Lukeino Formation, Tugen Hills, Kenya. *Revue de Paléobiologie, Genève*, *37*(2), 577–591.

Shellis, R., Beynon, A., Reid, D., & Hiiemae, K. (1998). Variations in molar enamel thickness among primates. *Journal of Human Evolution*, *35*(4-5), 507–522.

Silcox, M. (2001). *A Phylogenetic Analysis of Plesiadapiformes and Their Relationship to Euprimates and Other Archontans*. Unpublished Ph. D. The Johns Hopkins University.

Simpson, S. W., Kleinsasser, L., Quade, J., Levin, N. E., McIntosh, W. C., Dunbar, N., … Rogers, M. J. (2015). Late Miocene hominin teeth from the Gona paleoanthropological research project area, Afar, Ethiopia. *Journal of Human Evolution*, *81*, 68–82.

Skinner, M. M., Evans, A., Smith, T., Jernvall, J., Tafforeau, P., Kupczik, K., … others. (2010). Brief communication: Contributions of enamel-dentine junction shape and enamel deposition to primate molar crown complexity. *American Journal of Physical Anthropology*, *142*(1), 157–163.

Smith, A. L., Benazzi, S., Ledogar, J. A., Tamvada, K., Pryor Smith, L. C., Weber, G. W., … others. (2015). The feeding biomechanics and dietary ecology of *paranthropus boisei*. *The Anatomical Record*, *298*(1), 145–167.

Smith, T. M., Olejniczak, A. J., Tafforeau, P., Reid, D. J., Grine, F. E., & Hublin, J.-J. (2006). Molar crown thickness, volume, and development in South African Middle Stone Age humans. *South African Journal of Science*, *102*(11-12), 513–517.

Stansfield, E., Parker, J., & O'Higgins, P. (2018). A sensitivity study of human mandibular biting simulations using finite element analysis. *Journal of Archaeological Science: Reports*, *22*, 420–432.

Swindler, D. R., & Ward, S. (1988). Evolutionary and morphological significance of the deflecting wrinkle in the lower molars of the Hominoidea. *American Journal of Physical Anthropology*, *75*(3), 405–411.

Thiery, G., Guy, F., & Lazzari, V. (2017). Investigating the dental toolkit of primates based on food mechanical properties: Feeding action does matter. *American Journal of Primatology*, *79*(6), e22640.

Thipparthi, K., Kandalai, S., & Kiran, K. (2021). Effect of counterforts and buttresses on retaining wall using finite element analysis. In *IOP conference series: Materials science and engineering* (Vol. 1057, p. 012077). IOP Publishing.

Tobias, P. V. (1967). *Olduvai Gorge* (1st ed., Vol. 2). Cambridge: Cambridge University Press.

Vogel, E. R., Woerden, J. T. van, Lucas, P. W., Atmoko, S. S. U., Schaik, C. P. van, & Dominy, N. J. (2008). Functional ecology and evolution of hominoid molar enamel thickness: *Pan troglodytes schweinfurthii* and *pongo pygmaeus wurmbii*. *Journal of Human Evolution*, *55*(1), 60–74.

Vollmer, J., Mencl, R., & Mueller, H. (1999). Improved laplacian smoothing of noisy surface meshes. In *Computer graphics forum* (Vol. 18, pp. 131–138). Wiley Online Library.

Weidmann, S., Weatherell, J., & Hamm, S. M. (1967). Variations of enamel density in sections of human teeth. *Archives of Oral Niology*, *12*(1), 85–97.

Xing, S., Martinón-Torres, M., & Castro, J. M. B. de. (2018). The fossil teeth of the Peking Man. *Scientific Reports*, *8*(1), 2066.

Xing, S., Sun, C., Martinón-Torres, M., Castro, J. M. B. de, Han, F., Zhang, Y., & Liu, W. (2016). Hominin teeth from the Middle Pleistocene site of Yiyuan, eastern China. *Journal of Human Evolution*, *95*, 33–54.

Zhang, Y., Kono, R. T., Jin, C., Wang, W., Harrison, T., & others. (2014). Possible change in dental morphology in *gigantopithecus blacki* just prior to its extinction: Evidence from the upper premolar enamel-dentine junction. *Journal of Human Evolution*, *75*, 166–171.